communications earth & environment

A Nature Portfolio journal

Article

https://doi.org/10.1038/s43247-025-02208-1

Neglecting future sporadic volcanic eruptions underestimates climate uncertainty

Man Mei Chim[1,7] ✉, Thomas J. Aubry[2], Chris Smith[3,4] & Anja Schmidt[1,5,6]

Most climate projections represent volcanic eruptions as a prescribed constant forcing based on a historical average, which prevents a full quantification of uncertainties in climate projections. Here we show that the contribution of volcanic forcing uncertainty to the overall uncertainty in global mean surface air temperature projections reaches up to 49% in 2029, and is comparable or greater than that from internal variability throughout the 21st century. Furthermore, compared to a constant volcanic forcing, employing a stochastic volcanic forcing reduces the probability of exceeding 1.5 °C warming above pre-industrial level by at least 5% for high climate mitigation scenario, and enhances the probability of negative decadal temperature trends by up to 8%. Intermediate to high climate mitigation scenarios are particularly sensitive to the choice of future volcanic forcing implementation. We recommend the use of either a stochastic approach or prescribed constant forcing levels that sample volcanic uncertainty in future climate simulations.

Volcanic forcing of climate is an important natural driver of climate variability that can lead to climate responses on decadal to multi-decadal timescales[1–4]. Despite its importance in climate variability, the unpredictable nature of volcanic eruptions makes it difficult to account for future eruptions in climate projections.

The Coupled Model Intercomparison Project (CMIP) of the World Climate Research Programme oversees the experimental protocol from state-of-the-art global climate models and Earth System Models (ESMs)[5]. Within CMIP, the Scenario Model Intercomparison Project (ScenarioMIP) provides climate projections to 2100 (or beyond) under a wide range of potential future emissions scenarios ranging from very low to very high[6]. ESM projections from ScenarioMIP are a critical line of evidence that informs the Intergovernmental Panel on Climate Change (IPCC) Assessment Reports[7]. For the climate projections of the most recent intercomparison project (CMIP6), ScenarioMIP recommended prescribing a constant volcanic forcing with a magnitude equivalent to the 1850–2014 historical mean forcing values[6]. However, this approach has several limitations: (1) it does not consider the sporadic nature of volcanic eruptions and the variability of volcanic forcing in the future[4,8]; (2) it is biased by the under-recording of small-magnitude eruptions prior to 1978, the start of the satellite era[8]; (3) it poorly represents the long-term forcing of large-magnitude eruptions with a short time period between 1850 and 2014, and it does not account for eruptions larger in magnitude in terms of volcanic sulfur dioxide (SO_2) mass prior to 1850[4,8]. Consequently, the constant volcanic forcing approach does not allow for a full quantification of uncertainties resulting from sporadic volcanic eruptions in climate projections. Therefore, the combined uncertainty in climate projections is larger than can be expressed with the current CMIP6 ScenarioMIP design.

Hawkins and Sutton[9] identify three primary sources of uncertainties in climate projections, including model uncertainty, scenario uncertainty, and internal variability. Model uncertainty stems from the differences between the responses of climate models to identical forcings. Scenario uncertainty relates to different future anthropogenic emissions and warming pathways. Internal variability refers to the decadal and sub-decadal fluctuations around the mean climate states due to internal natural processes such as the El Niño-Southern Oscillation and Pacific Decadal Oscillation. Apart from these three sources of uncertainties, recent studies using a stochastic forcing approach show that natural forcings like volcanic eruptions can potentially introduce large additional uncertainties in climate projections[4,8]. Bethke et al.[4] first demonstrate the importance of representing volcanic forcing uncertainty in climate projections using a stochastic volcanic forcing approach, in which they generate 60 forcing members by resampling from a

[1]Centre for Atmospheric Science, Yusuf Hamied Department of Chemistry, University of Cambridge, Cambridge, United Kingdom. [2]Department of Earth and Environmental Sciences, University of Exeter, Penryn, United Kingdom. [3]Department of Water and Climate, Vrije Universiteit Brussel, Brussels, Belgium. [4]International Institute for Applied Systems Analysis, Laxenburg, Austria. [5]German Aerospace Center (DLR), Institute of Atmospheric Physics, Oberpfaffenhofen, Germany. [6]Meteorological Institute, Ludwig-Maximilians University Munich, Munich, Germany. [7]Present address: Department of Mathematics and Statistics, University of Exeter, Exeter, United Kingdom. ✉e-mail: m.m.chim@exeter.ac.uk

2500-year ice core record. Building on this methodology, Chim et al.[8] enhance the approach by considering eruptions of both large- and small-magnitudes with an expanded dataset combining ice-core and satellite observations spanning the past 11,500 years. Using the improved volcanic forcing approach, Chim et al.[8] show that CMIP6 ScenarioMIP very likely underestimates the magnitude of future volcanic forcing and the associated climate effects. However, the use of only four volcanic forcing scenarios in Chim et al.[8] and the biased eruption frequency-magnitude distribution in Bethke et al.[4] means that the contribution of uncertainty associated with volcanic eruptions has not yet been fully quantified in climate projections. These studies are limited to using a single model and a single anthropogenic forcing scenario due to the high computational cost of ESMs, which prevents a full quantification of uncertainty contributions across different climate models, volcanic futures, and anthropogenic forcing scenarios.

Large-magnitude volcanic eruptions can cause sudden global surface cooling that lasts for at least 1–2 years[10]. However, climate projections that use a constant volcanic forcing cannot capture the sudden surface cooling caused by large-magnitude volcanic eruptions. Not only do these large-magnitude eruptions induce climate impacts, but can also pose threats to agriculture and have long-lasting socio-economic impacts. For example, the 1815 Mt. Tambora eruption, which injected 56 Tg ± 9 Tg of SO_2 into the stratosphere according to the eVolv2k ice-core based volcanic emission dataset[11], led to a 0.8 °C drop in global surface temperature, regional cooling up to 4 °C over Europe, and suppressed rainfall over Southeast Asia[12–14]. The climatic changes of the 1815 Mt. Tambora eruption caused crop failures and famine across Europe, North America and China[13,15]. Ice core records from Sigl et al.[16] suggest that the chance of having an eruption with volcanic SO_2 emissions at least as large as the 1815 Mt. Tambora eruption is 16.5% in the 21st century. To assess the climate risks and socio-economic impacts of these large-magnitude eruptions in the future, it is necessary to account for the sporadic nature of volcanic forcing in climate projections.

Here, we isolate and quantify the contribution of volcanic uncertainty in climate projections by simulating 1000 stochastic volcanic forcing scenarios using a simple volcanic aerosol model[17,18] and the Finite-amplitude Impulse Response (FaIR) climate model[19,20]. We generate stochastic volcanic SO_2 emission scenarios from ice core and satellite records spanning over the past 11,500 years and convert them to stochastic volcanic forcing scenarios (see Methods Sections "Design of stochastic volcanic emission scenarios", "Aerosol optical properties and effective radiative forcing" and "Simulation design"). We project global mean surface air temperature (GMSAT) from 2015 to 2100 under three shared socio-economic pathways (SSPs) representing very low (SSP1-1.9), intermediate (SSP2-4.5), and very

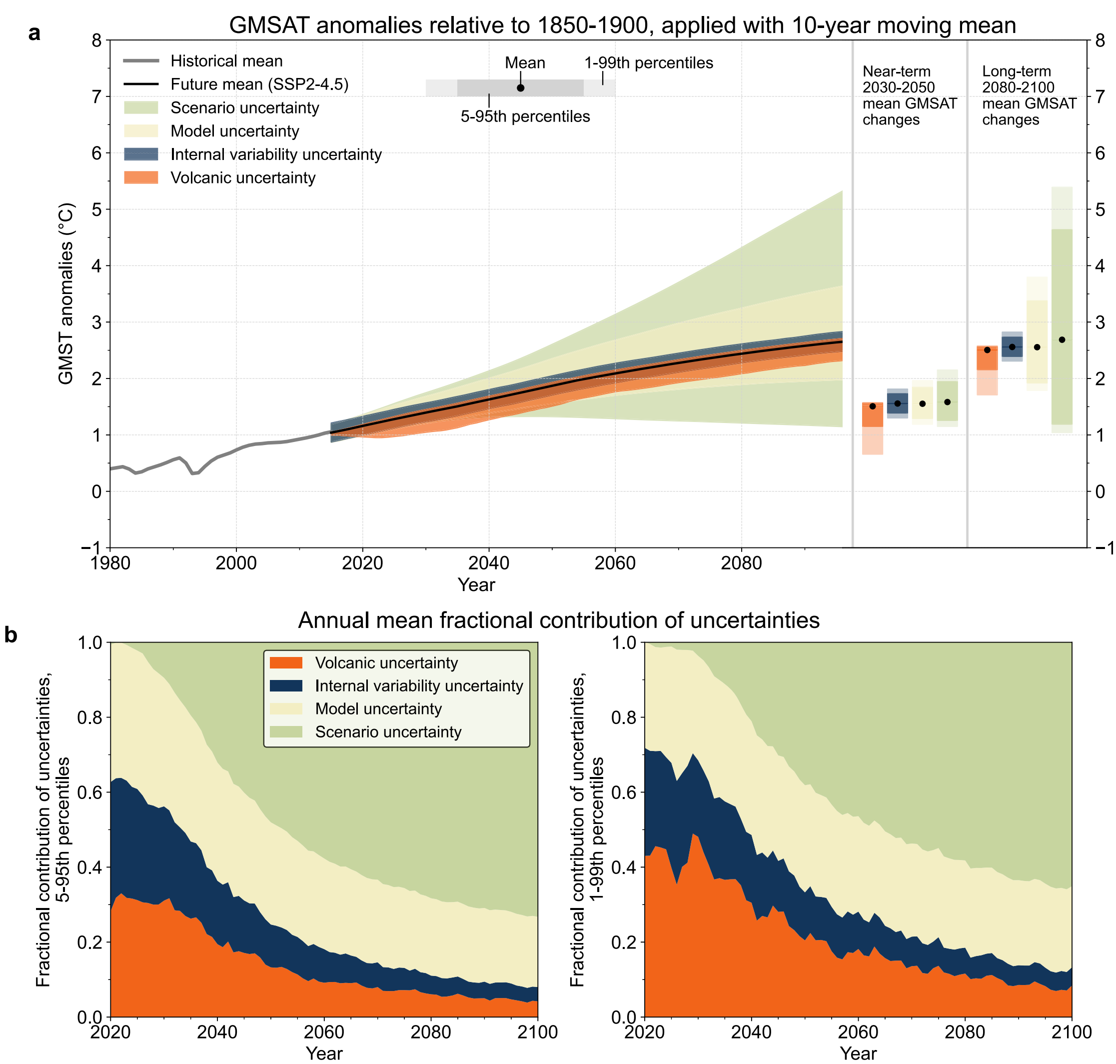

Fig. 1 | Contribution of volcanic forcing uncertainty to overall uncertainties in global mean surface air temperature projections. a Projections of global mean surface air temperature (GMSAT) anomalies relative to 1850–1900 from FaIR model simulations, applied with 10-year moving mean. The shaded regions show the 5th to 95th percentiles of the uncertainties. The boxplots show the near-term (2030–2050) and long-term (2080–2100) mean GMSAT changes. **b** Annual mean fractional contribution of the uncertainties from 2020 to 2100 for the 5th to 95th percentiles (left) and 1st to 99th percentiles (right).

high (SSP5-8.5) emissions scenarios. The FaIR model is calibrated to emulate the climate response of a range of CMIP6 models and takes into account the uncertainty of internal variability[20] (see Methods Section "FaIR model description"). It shows excellent performance in simulating volcanic cooling over the last 750 years as compared to tree ring-based recontructions[21]. We assess the role of volcanic uncertainty in the probability of exceeding 1.5 °C, 2 °C and 3 °C warming thresholds, and the probability of short-term surface cooling by 2100 (see Methods Section "Calculation of uncertainties and probabilities").

Our results show that the contribution to uncertainty associated with volcanic forcing is comparable to that from internal variability on temperature projections throughout the 21st century. Future stochastic volcanic forcing reduces the probability of exceeding warming thresholds (i.e., 1.5 °C, 2 °C and 3 °C) to varying extents across the three SSPs. The standard CMIP6 approach using a constant volcanic forcing greatly underestimates the probability of short-term surface cooling. The use of stochastic volcanic forcing is necessary to assess the socio-economic impacts and risks of future volcanic eruptions. We suggest an improved magnitude of volcanic forcing in future ScenarioMIP iterations to account for the contributions from both small-magnitude eruptions and larger-magnitude eruptions.

Results and discussion

Large contribution of volcanic forcing to uncertainties on temperature projections

Figure 1 shows the projection of GMSAT anomalies relative to the 1850–1900 period simulated by the FaIR model and its uncertainties (see Methods for uncertainty calculations). Volcanic uncertainty contributes significantly to overall uncertainties in climate projections, accounting for up to 33% (5th–95th percentile) in 2022 and 49% (1st-99th percentile) in 2029 of the total uncertainty in the initial 15 years (Fig. 1b). This contribution is comparable to that of internal variability which accounts for up to 34% (5th–95th percentile) and 29% (1st–99th percentile) in 2020. Volcanic forcing uncertainty ramps up in the initial 5–6 years before reaching values representative of the true volcanically-driven uncertainty on GMSAT across our simulations. This ramp up is due to: i) the typical aerosol lifetime of about 2–3 years; and ii) the timescale of the climate response to volcanic forcing of about 5–10 years in FaIR[21]. Beyond the ramp up period, volcanic forcing uncertainty systematically exceeds internal variability from year 2022 (5th–95th percentile) and year 2018 (1st–99th percentile) onwards. Together, volcanic forcing and internal variability dominate projection uncertainties for at least a decade, extending to 2033 (5th–95th percentile) or 2038 (1st–99th percentile) (Fig. 1b). When accounting for volcanic uncertainty, the 2030–2050 mean GMSAT changes are projected to be 1.5 °C above 1850-1900 levels. The volcanic uncertainty has a distribution skewed towards cooling, with a 5th–95th percentile range between 1.2 °C and 1.6 °C, and a 1st–99th percentile range between 0.7 °C and 1.6 °C (Fig. 1a).

Although volcanic eruptions are sporadic in nature, the volcanic uncertainty remains constant in projections when averaged with a 10-year moving mean (Fig. 1a). As scenario and climate uncertainties increase significantly over time, their fractional contributions dominate the overall uncertainties in the longer term (Fig. 1a, b). In the long-term future (2080–2100), the mean GMSAT changes accounting for volcanic uncertainty is projected to be 2.5 °C with a 5th–95th percentile range of 2.2–2.6 °C, and a 1st-99th percentile range of 1.8–2.6 °C relative to 1850–1900. By 2100, the fractional contribution of volcanic uncertainty is estimated to be between 4.0% (5th–95th percentile) and 8.0% (1st–99th percentile), compared to 3.6% (5th–95th percentile) to 4.6% (1st–99th percentile) from internal variability (Fig. 1b).

Stochastic volcanic forcing scenarios delay crossing 1.5 °C

Improving the representation of volcanic forcing with stochastic emission scenarios reduces the probability of exceeding the 1.5 °C warming threshold for all the three SSP scenarios in the near-term future (Fig. 2a). We find that in the near-term future between 2030 and 2050, the differences in probability of 1.5 °C exceedance between projections using stochastic forcings and historically-averaged forcing is 5–7% for SSP1-1.9, 4–10% for SSP2-4.5, and 0–9% for SSP5-8.5 (Fig. 2b). The higher forcing magnitude in stochastic forcing compared to the historically-averaged forcing in CMIP6 ScenarioMIP leads to, on average, a reduced probability of exceeding warming thresholds. Our finding confirms the results in Chim et al.[8], which on the basis of three forcing scenarios and the UKESM climate model, suggested that stochastic volcanic forcing scenarios lead to reduced GMSATs and delay the crossing of the 1.5 °C, 2 °C and 3 °C warming thresholds by 2–7 years.

In the long term, warming levels in high-end SSP scenarios are sufficiently high that the probability of exceeding 1.5 °C is 100% within this century regardless of the implementation of stochastic volcanic forcings. For our low-end SSP scenario (i.e., SSP1-1.9), our simulation with stochastic volcanic forcings consistently reduces the probability of crossing 1.5 °C by about 5% throughout the 21st century. The choice of volcanic forcing implementation in climate projection is therefore particularly important for a low warming threshold of 1.5 °C and low-end SSP scenarios (e.g., SSP1-1.9), which are expected to be an important focus of CMIP7 ScenarioMIP[22].

In contrast to the 1.5 °C warming threshold, the choice of volcanic forcing implementation has a smaller effect on the probabilities of exceedance for higher warming thresholds of 2 °C and 3 °C, in particular for SSP1-1.9 (Supplementary Figs. S1 and S2). The difference in probabilities of exceedance is up to 1% for SSP1-1.9, and 6-7% for SSP2-4.5 and SSP5-8.5 for a warming threshold of 2 °C (Supplementary Fig. S1). As the low-end SSP scenario has a lower level of warming, the effect of stochastic volcanic forcing is smaller for SSP1-1.9 than the higher SSP scenarios.

Although inclusion of a stochastic volcanic forcing in future scenarios reduces the likelihood of single years crossing 1.5 °C, compliance with Paris Agreement thresholds should be assessed using long-term trends of the anthropogenic component of warming[23,24].

Increased likelihood of abrupt surface cooling using stochastic volcanic forcings

Figure 3a and Supplementary Fig. S3 illustrate the probability of at least one occurrence of a short-term (one-year and two-year) GMSAT reduction greater than temperature thresholds between 0.1 °C and 0.9 °C by 2100. The historically-averaged (constant) forcing approach, where GMSAT variability arises from internal variability but not volcanic forcing, underestimates the probability of one-year and two-year short-term cooling (Fig. 3a and Supplementary Fig. S3). The peak global-mean surface cooling of the 1991 Mt. Pinatubo eruption was about 0.29 °C (uncertainty range: 0.21–0.37 °C), calculated using the Volc2Clim tool[25] (See Methods "Calculation of uncertainties and probabilities"). There is a 50–70% chance (depending on SSP scenarios) of having at least a one-year GMSAT reduction of 0.3 °C by 2100 using stochastic forcings, as compared to a 5–15% chance using a historically-averaged forcing.

For a peak cooling greater than 0.45 °C, the probability is <1% in the simulations with constant volcanic forcing, compared to a 35% to 45% probability in simulations with stochastic volcanic forcing (Fig. 3a). For a Mt. Tambora-like eruption with peak cooling of about 0.85 °C, historically-averaged forcing gives a zero probability, while using a stochastic forcing gives a probability of about 5%. Furthermore, defining short-term cooling as the mean GMSAT reduction over two consecutive years exceeding specific temperature thresholds reveals more pronounced differences between constant and stochastic volcanic forcing approaches. While the constant forcing approach results in a zero probability for two-year GMSAT reduction greater than 0.25 °C for all three SSP scenarios, the stochastic forcing approach indicates at least a 41% probability of reaching the 0.25 °C temperature threshold. The probability of short-term cooling is lower in weaker climate mitigation scenarios because higher rates of warming offset some of the volcanic cooling.

The use of a constant volcanic forcing leads to a narrower distribution of decadal temperature trend, underestimating the probability of both extreme warm and cold periods (Fig. 3b). Bethke et al.[4] show that the

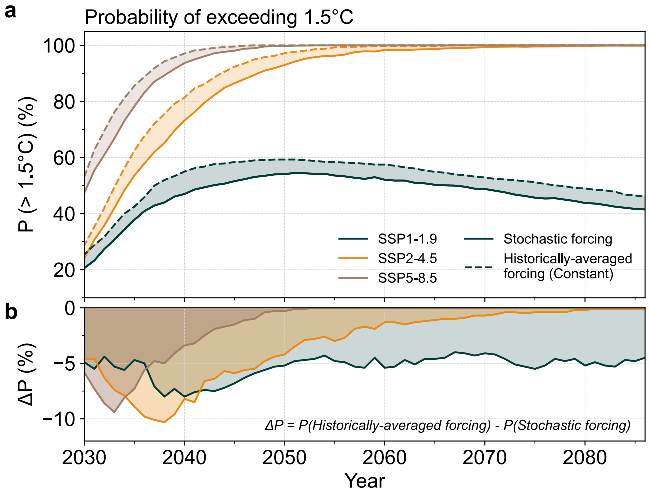

Fig. 2 | Probability of exceeding 1.5 °C with stochastic versus constant volcanic forcing approaches. **a** Probability of scenarios exceeding 1.5 °C using stochastic volcanic forcing (solid lines) and 1850–2014 mean historically-averaged forcing (dotted lines) for SSP1-1.9, SSP2-4.5 and SSP5-8.5 scenarios. **b** The difference in probability in exceeding 1.5 °C between the simulations with historically-averaged (constant) forcing and stochastic volcanic forcing (see Methods Section "Calculation of uncertainties and probabilities").

probability of the occurrences of negative decadal trends (<0 °C per decade) increases from 10% for zero volcanic forcing, to more than 16% for stochastic volcanic forcing for an intermediate future anthropogenic emission scenario (Representative concentration pathway, RCP4.5). Our simulation with a comparable future anthropogenic emission scenario (i.e., SSP2-4.5) shows a slightly higher increase in the probability of negative decadal trends from 10% for constant volcanic forcing, to 18% when accounting for stochastic volcanic forcing (Supplementary Fig. S4), which agrees well with Bethke et al.[4] for the NorESM model and RCP4.5 scenario. The higher probability of negative decadal trends in our simulation likely arises from the wider range of stochastic volcanic forcings and climate system uncertainties used. Our results show that the probability of having negative decadal trends is dependent on the future emission scenario. For instance, the probability of having negative decadal trends is similar (43–44%) between constant and stochastic volcanic forcings for SSP1-1.9, and the probability increases from 1% to 6% for SSP5-8.5 (Supplementary Fig. S4). Our simulations using constant volcanic forcing also overestimate the probability of warming decadal trends exceeding 0.5 °C by 4–7% across the SSP scenarios.

In addition to surface cooling events, Supplementary Fig. S5 illustrates the probability of at least one occurrence of a short-term GMSAT increase greater than the temperature thresholds between 0.1 and 0.9 °C by 2100. Despite leading to lower temperature projections, the simulations using stochastic volcanic forcing increase the probability of short-term warming occurrence than the constant volcanic forcing for the entire range of temperature thresholds. Our results highlight that the use of a constant volcanic forcing neglects abrupt warming and cooling events and leads to a bias in GMSAT distribution as compared to using a stochastic volcanic forcing.

Improving future volcanic forcing in climate projections

Our model results show that stochastic volcanic forcing can lead to large uncertainties on temperature projections, in particular during the initial decades. However, to account for volcanic uncertainties in future climate modelling experiments (i.e., CMIP), it is infeasible to simulate a thousand stochastic forcing scenarios using the computationally expensive ESMs.

Figure 4 shows the probability density function of stratospheric aerosol optical depth (SAOD) for the 1000 stochastic scenarios, and the corresponding temperature projections under SSP2-4.5 for the 5th, 50th and 95th percentiles of the SAOD distribution. The 2015–2100 averaged GMSAT of the constant median forcing is 0.03 °C lower than the CMIP6 forcing, which is consistent with the results in Chim et al.[8], but not as low as the values in Chim et al.[8] simulated by the UKESM1 climate model (between 0.08 and 0.12 °C). The difference in GMSAT potentially arises from the higher SAOD values in Chim et al.[8] than our study (Fig. 4a), and the high climate sensitivity in the UKESM1 model[26]. Supplementary Table S1 shows the time-averaged SAOD values calculated using the idealised volcanic forcing emulator, Easy Volcanic Aerosol (EVA_H), and UKESM1 for the stochastic scenarios simulated. In our study, the median of the 2015–2100 time-averaged SAOD of the stochastic scenarios is 0.0138 (5th–95th percentile range: 0.0072–0.0296), which is about 22% greater than the 1850–2014 mean value (0.0107) used in CMIP6 ScenarioMIP (Fig. 4a and Supplementary Table S1). The median of 2015–2100 time-averaged SAOD in our study calculated using EVA_H is 45% lower than that simulated by UKESM in Chim et al.[8]. The difference in the SAOD values can be explained by the aerosol model sensitivity to volcanic forcing. Clyne et al.[27] demonstrated that for a Mt. Tambora-like eruption, UKESM1 simulates a higher SAOD than EVA, with EVA_H simulating slightly lower SAOD than EVA, in particular for extratropical eruptions[18]. The FaIR model, calibrated with the CMIP6 model results and constrained to the assessment of climate sensitivity in AR6[20,28], is expected to simulate a smaller GMSAT response in the median compared to UKESM1, which exhibits higher climate sensitivity. Supplementary Fig. S6 demonstrates that when FaIR is calibrated with UKESM1, the GMSAT responses between the two models become comparable. Last, Fig. 4a also shows the mean SAOD value of the CMIP7 dataset accounting for small-magnitude eruptions. The CMIP7 1850–2014 mean SAOD (0.014) is the same as the median of our stochastic scenarios, and 27% larger than the CMIP6 1850-2014 mean SAOD (0.011).

The current forcing approach in ScenarioMIP underestimates the climate uncertainty arising from future volcanic eruptions (Fig. 1), which potentially lead to biased mean climate in projections. We find that the GMSAT projection of the median of the stochastic scenarios is comparable to that of the constant median forcing of the SAOD distribution (Fig. 4b). This shows that the use of a constant volcanic forcing equivalent to the 50th percentile of the SAOD distribution is a good estimation of the median of the future GMSAT projection across the 1000 stochastic scenarios. We do not recommend a stochastic volcanic forcing approach in ScenarioMIP because it is computationally expensive to implement for multiple ESMs and future anthropogenic forcing scenarios. However, we suggest that the Reduced Complexity Model Intercomparison Project could consider an experiment with a large number of volcanic scenarios for full uncertainty quantification[29]. To improve the representation of volcanic forcing in climate projections, we suggest future ScenarioMIP experiments prescribe a constant volcanic forcing that accounts for the contribution of small-magnitude eruptions, e.g., a historically-averaged mean that considers the missing SO_2 flux from small-magnitude eruptions prior to 1978 (i.e., a 1850-2014 time-averaged value of 0.014 in the CMIP7 dataset), or the 50th percentile of SAOD distribution (i.e., a 2015–2100 time-averaged value of 0.014) based on stochastic scenarios resampled from the latest ice-core and satellite volcanic emission record. This approach improves the magnitude of future volcanic forcing and the mean climate state in climate projections. In order to quantify the contribution of volcanic uncertainty on climate projections, we suggest modelling groups perform projections with constant volcanic forcings at the 5th and 95th percentiles of the SAOD distribution of the stochastic scenarios.

The recommendation of a constant volcanic forcing approach, however, fails to fully account for climate variability and constrains our ability to fully assess the distribution of GMSAT (Fig. 3, Supplementary Figs. S3 and S4) and other key climate indicators[4,8]. The effects of large-magnitude eruptions are not limited to surface temperature changes. Large-magnitude eruptions can also pose a threat to infrastructure, agriculture, and energy supply[30], which themselves lead to socio-economic shocks and the potential for reduced economic productivity that may feed back into emission scenarios and eventually to climate projections, an effect not investigated in this study. The use of stochastic volcanic forcings in climate models and projections is necessary to allow the assessment of the abrupt climatic changes caused by large-magnitude volcanic eruptions, and the associated climatic risks and

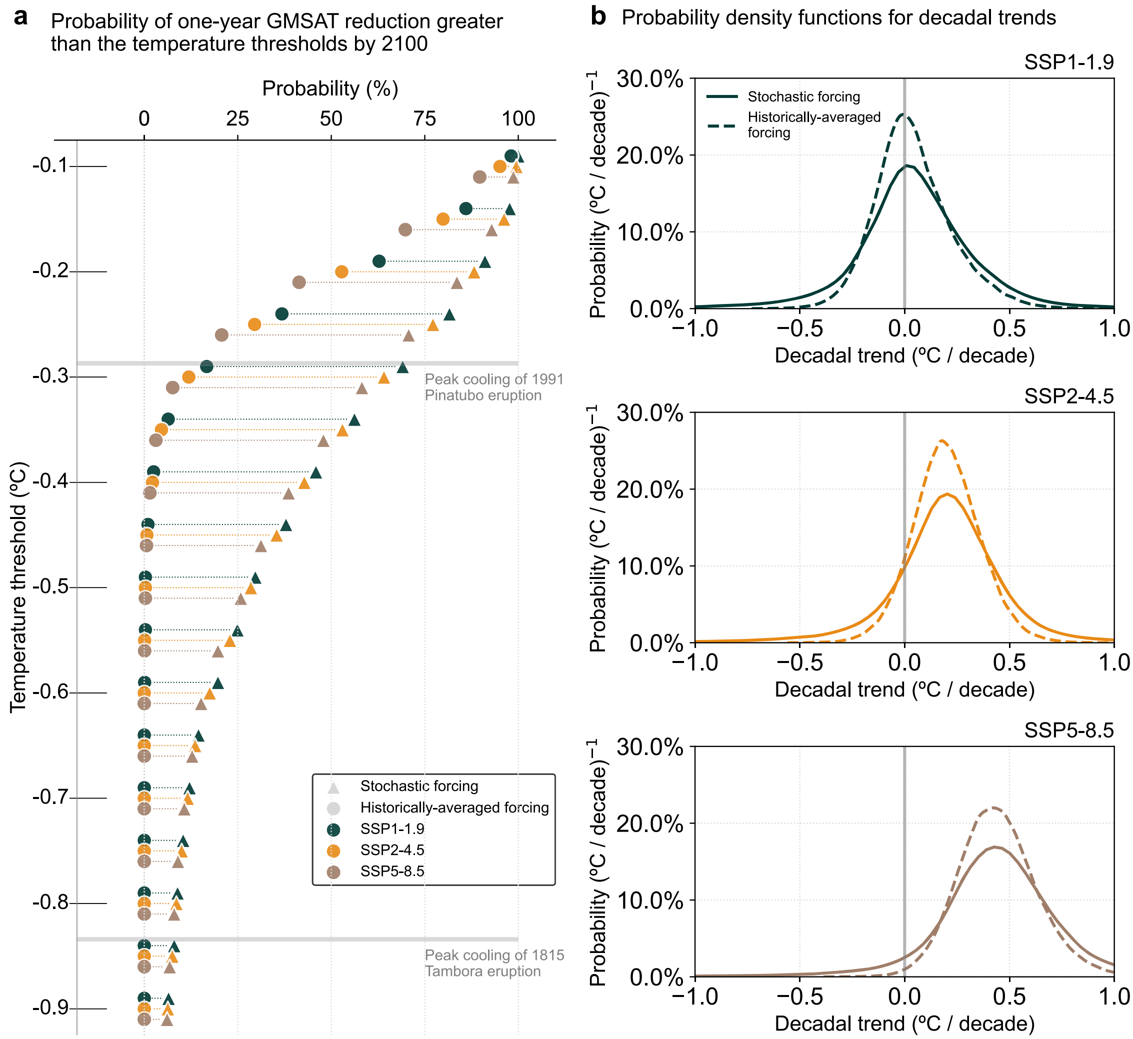

Fig. 3 | Probabilities of one-year and decadal temperature cooling trends with and without stochastic volcanic forcing. a Probability of at least one occurrence of one-year global mean surface air temperature (GMSAT) reduction greater than the shown temperature thresholds for the three SSP scenarios. **b** Probability density functions for decadal GMSAT trends (in °C per decade), calculated using a 10-year moving window, for the three SSP scenarios.

socio-economic impacts. In addition, future climate warming modulates the climate effects of volcanic sulfate aerosols via climate-volcano feedbacks[31]. We encourage individual modelling groups to perform climate projection experiments using a stochastic volcanic forcing approach similar to Bethke et al.[4] and Chim et al.[8] to fully assess the climate and socio-economic feedbacks associated with future volcanic eruptions.

In addition to future volcanic eruptions, the uncertainties associated with other forcings, such as wildfires, on climate projections remains unanswered. Future studies could apply the methodology developed in our study to examine the uncertainties of these forcings on climate projections.

Methods

Design of stochastic volcanic emission scenarios

The stochastic volcanic sulfur dioxide (SO_2) emission scenarios we use are those described in detail in Chim et al.[8] and we briefly summarise their design here. Chim et al.[8] generate an ensemble of 1000 scenarios spanning the years 2015–2100 by independently resampling:

i. Small-magnitude eruptions (<3 Tg of SO_2) from the 1979–2021 satellite record[32], which captures stratospheric volcanic SO_2 emissions from eruptions of all magnitudes and is much longer than the typical return period of small-magnitude eruptions (months to years).
ii. Large-magnitude eruptions (≥3 Tg of SO_2) from the combined 9496 BCE to 1978 CE ice-core records[16] and the 1979–2021 satellite record[32].

Chim et al.[8] do not resample small-magnitude eruptions from the ice-core record because injections much smaller than 10 Tg of SO_2 are poorly detected in ice cores. The maximum eruption size in the ice-core record Chim et al.[8] use is 378 Tg of SO_2, but we expect the dataset to only reasonably capture the frequency-magnitude distribution of eruptions injecting up to a maximum of ≃100 Tg of SO_2, with return periods less than 1000 years which is much shorter than the 11,500 years dataset coverage. The scenarios for small- and large-magnitude eruptions are then combined into a single scenario. Both magnitudes of eruptions significantly contribute to the long-term volcanic forcing[8].

The timing of each eruption is randomly resampled within 2015–2100. The eruption location and injection height are that from the satellite record if the eruption is resampled from this record. For eruptions resampled from the ice-core record, the broad latitudinal region (i.e., southern extratropical, tropical or northern extratropical) is inferred based on the sulfate deposition ratio between Greenland and Antarctica, and an exact volcano within these regions is resampled from the Smithsonian Global Volcanism Program Holocene Eruption database[33]. The injection height is either that reconstructed from the geological record or, in the vast majority of cases where it is unknown, it is assumed to be 25 km above sea level (the same as that of the 1991 eruption of Mt. Pinatubo[34]).

The result is an ensemble of 1000 scenarios for the mass, timing, altitude and latitude of volcanic SO_2 injection for 2015–2100. These

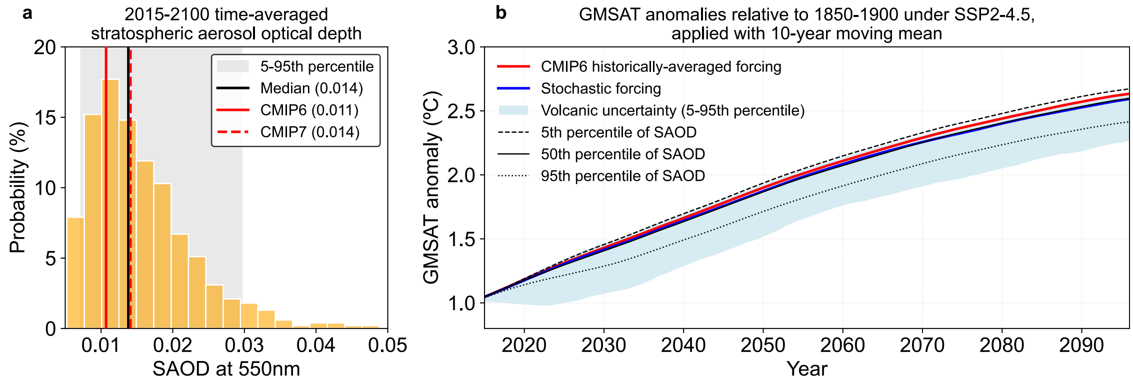

Fig. 4 | Global mean surface air temperature projections under different constant volcanic forcing magnitudes. a Probability density function of the 2015–2100 time-averaged mean stratospheric aerosol optical depth (SAOD) of the 1000 stochastic scenarios. The CMIP6 ScenarioMIP 1850–2014 time-averaged SAOD mean value (0.011) is denoted as red line. The CMIP7 1850–2014 time-averaged SAOD mean value (0.014) is denoted as red dotted line; it is obtained from the CMIP7 version 2.0.0 dataset available on Earth System Grid Federation. The median (0.014) and 5th–95th percentile of the ranked SAOD across 1000 stochastic scenarios are denoted as black line and grey shading, respectively. **b** Global mean surface air temperature (GMSAT) anomaly (°C) relative to 1850–1900 under SSP2-4.5, applied with 10-year moving mean. The blue line shows the median of the 1000-member stochastic volcanic forcing, and the blue shading shows the range of 5th−95th percentile with volcanic uncertainty only. The red line shows the median of GMSAT projection using the CMIP6 1850-2014 historical mean forcing. The black lines show the median of GMSAT projections for the 5th, 50th and 95th percentiles of the SAOD distribution.

scenarios are consistent with state-of-the-art eruption inventory records in terms of space-frequency-magnitude eruption distribution, and are expected to capture this distribution well for eruption magnitudes smaller than on the order of 100 Tg of SO_2[8]. Note that our scenarios ignore the potential impacts of climate change on eruption distribution space-frequency-magnitude[35] or on the height at which volcanic plumes inject SO_2 into the atmosphere[36].

Supplementary Fig. S7 shows the annual SO_2 flux of the 1000 stochastic scenarios. Based on the current volcanic SO_2 emission records, the 1850–2014 averaged volcanic SO_2 flux ranges between 0.77 to 0.86 Tg of SO_2 per year[3,32,37,38], as compared to 1.44 Tg of SO_2 per year for the median stochastic scenario. The CMIP7 volcanic SO_2 emission inventory, which complements bipolar ice-core record pre-satellite era with the D4i high-resolution Greenland record[39] and geological records of small-magnitude eruptions (Global Volcanism Programme Volcanoes of the World database) has a 1850–2021 averaged volcanic SO_2 flux of 1.0 Tg SO_2 per year. UKESM model simulations from Chim et al.[8] showed that the 2015–2100 time-averaged SAOD ranged between 0.015 to 0.062 using the low-end (2.5th percentile) and high-end (97.5th percentile) stochastic scenarios, as compared to a value of 0.012 for a constant volcanic forcing following the ScenarioMIP design.

Supplementary Fig. S8 shows the distribution of the eruption location for all the eruptions in the 1000 stochastic volcanic emission scenarios. The ratio of southern extratropical: tropical: northern extratropical eruptions for the median stochastic scenario is 0.04: 0.46: 0.5. In the historical volcanic emission datasets that we used in this study, the eruption location ratio is 0.06: 0.48: 0.46 for large-magnitude eruptions (>3 Tg of SO_2) and 0.05: 0.46: 0.50 for small-magnitude eruptions (<3 Tg of SO_2). Since the stochastic scenarios are resampled from the ice-core and satellite-based volcanic emission datasets, it is expected that the ratio of their latitudinal distribution is similar.

Supplementary Fig. S9 shows the distribution of eruption months/season for the 1000 stochastic scenarios. The distributions are similar across the four different categories of eruption months.

Out of the 1000 stochastic scenarios, there are 564 scenarios that have at least one double-eruption event, which is defined as having two large-magnitude eruption (>3 Tg of SO_2) occurring within three years of each other. If we consider eruptions with SO_2 injection greater than 15 Tg of SO_2, there are 71 scenarios that have at least one double-eruption event.

Aerosol optical properties and effective radiative forcing

To obtain a 2015–2100 effective radiative forcing time series for each of our volcanic emission scenarios, we first use the simple EVA_H volcanic aerosol model[18]. EVA_H uses input SO_2 injection parameters (mass, date, altitude and latitude) to produce 4-D (latitude, altitude, time and wavelength) aerosol optical properties. EVA_H is a simple box model where the stratosphere is divided in three latitudinal and three altitude bands, and where aerosol production, loss and transport processes are parameterized using constant timescales[18]. It builds on Easy Volcanic Aerosol[40], which was extensively used in CMIP6 VolMIP[41] and PMIP[42]. Unlike EVA, EVA_H accounts for the role of volcanic injection latitude and altitude in determining aerosol optical properties. One of the main limitations is that EVA_H overestimates the lifetime of sulfate aerosol produced by small-magnitude volcanic eruptions[43]. However, given the large uncertainty in interactive stratospheric aerosol models, simple models like EVA_H represent a reasonable middle-ground estimate of the aerosol optical property response to volcanic SO_2 injection[27]. Furthermore, the model simplicity makes it feasible to simulate 86,000 years (1000 stochastic scenarios from 2015 to 2100) of volcanic injections.

Using the global mean 550 nm stratospheric aerosol optical depth (SAOD) time series from EVA_H, we then follow Marshall et al.[17] to estimate the global mean effective radiative forcing (ERF) as:

$$ERF = -20.7 \times (1 - \exp(-\Delta SAOD)) \tag{1}$$

where ΔSAOD is the difference between the global mean 550 nm SAOD and its minimum over the historical period. The relationship shown in Eq. (1) is calibrated using the UM-UKCA interactive stratospheric aerosol model with an extensive set of stratospheric aerosol injection simulations, which includes 82 explosive eruptions with different eruption source parameters (i.e., SO_2 emission, eruption latitude, and the emission height)[17]. The use of a non-linear relationship better reflects the physical relationship expected between radiative forcing and SAOD as opposed to a linear relationship (e.g., Schmidt et al.[44]). Equation (1) also leads to a forcing 20–25% smaller than the one estimated in Intergovernmental Panel on Climate Change fifth assessment report (IPCC AR5)[45] for the same SAOD, primarily as a result of accounting for rapid adjustments modulating the radiative forcing[17]. According to the IPCC AR6, the radiative forcing of volcanic aerosols follows a linear relationship of -20 ± 5 W/m^2 per unit of SAOD, which yields a magnitude similar to that given by Eq. (1), particularly for smaller forcings[28].

Although the relationship between SAOD and ERF varies in time and for instance with eruption latitude and season[17], we use the same relationship for all eruptions because we model 86-year eruption sequences as opposed to individual eruptions for which we could use relationships specific to the eruption latitude or season considered[17]. Altogether, the sequential use of EVA_H and Eq. (1) enable us to calculate the 2015–2100 global mean volcanic aerosol ERF time series for each of the 1000 stochastic emission scenarios used. As with the emission scenarios, we ignore the potential impacts of climate change on volcanic aerosol processes and resulting radiative forcing[31]. Supplementary Table S1 provides the ΔSAOD and ERF values used in our simulations. Supplementary Fig. S6 shows the comparison between the SAOD, ERF and GMSAT projections simulated by FaIR and UKESM1.1 for three stochastic scenarios (at the 2.5th, 50.0th and 98.0th percentile, as in Chim et al.[8]) under SSP3-7.0.

FaIR model description

To calculate the 2015–2100 GMSAT for various volcanic and anthropogenic forcing scenarios, we use the Finite-amplitude Impulse Response (FaIR) model. FaIR is a reduced-complexity climate model that produces GMSAT projections from inputs of anthropogenic emissions and effective radiative forcing[19,46]. FaIR includes emissions of 51 anthropogenic emissions categories spanning the most important greenhouse gases and aerosol and ozone precursor species. Natural forcings from solar variability and volcanic activity are provided as external time series. In this study we use FaIR version 2.1.4[19,20].

FaIR includes simplified representations of the carbon and methane cycles, including carbon cycle feedbacks[47] and the effect of chemically-active greenhouse gases and short-lived climate forcers on methane lifetime[48]. Concentrations of greenhouse gases other than CO_2 and CH_4 are modelled with a single invariant atmospheric lifetime based on the most recent IPCC assessment[49,50]. Effective radiative forcing from greenhouse gases is determined from well-established curve-fits to their concentrations[42]. Aerosol and ozone effective radiative forcings are also modelled from precursor emissions and their interactions as represented in CMIP6 models[49,51–53]. Minor forcing categories such as surface albedo from land use change and black carbon deposition on snow, contrails from aviation, and stratospheric water vapour from methane oxidation are calculated from emissions or concentrations of emitted species[46].

When the internal variability is switched on in the FaIR model, the model uses a stochastic internal variability which generates a stochastic component of the total effective radiative forcing[54]. This is based on CMIP6 models, and we include the autocorrelation in internal variability therefore simulating realistic fluctuations in GMSAT, such as clustering of warm and cool years in the El Niño-La Niña cycle (to the extent that CMIP6 models simulate these well). When the internal variability is switched off, the model reflects only directly forced effects (i.e., anthropogenic and natural forcings, including the stochastic volcanic forcing), on GMSAT.

We produce a 1000-member ensemble of FaIR that samples the uncertainty in climate response as calibrated against CMIP6 models and constrained to observations of historical climate change (GMSAT 1850–2022, ocean heat content 1971–2022, year 2022 CO_2 concentration from Forster et al.[55]) and assessments of key climate metrics (equilibrium climate sensitivity, transient climate response, direct, indirect and total aerosol forcing) from the IPCC AR6[28]. In this study we use fair-calibrate v1.4.2[56]. The calibration process ensures that all projections are historically consistent and in line with (though sampling the full range of uncertainty from) climate observations or the IPCC AR6. This calibration of FaIR uses the CMIP6 historical and future SSP emissions from the Reduced Complexity Model Intercomparison Project[29,57]. As the SSPs diverge from the historical in 2014, we use SSP2-4.5 as the scenario to fill the 2015–2022 period in the calibration and for comparison to recent climate observations. In this calibration dataset, we also follow the CMIP6 guidelines for extending volcanic forcing beyond the end of the historical period for the calibration, by ramping down the volcanic forcing in 2014 to the CMIP6 historical average over 10 years[5].

As part of the sampling process of FaIR, we also sample the conversion factor between SAOD and ERF from volcanic forcing, which has a 5–95% uncertainty range of ±25% around the best estimate value[58] which is applied as a direct scaling factor to Eq. (1).

The FaIR model parameters are constrained using the historical GMSAT observations between 1850 and 2022 from Forster et al.[28,55]. In the calibration of the FaIR model, Smith et al.[20] used two steps to constrain the model projection with historical values. The first step is to compare the FaIR ensemble members' root mean squared (RMSE) difference in GMSAT anomaly to the historical observed values, and reject the ensemble members with a RMSE difference greater than 0.17 °C. The second step is to reweight this first posterior to fit eight distributions of observed or assessed climate indicators, including equilibrium climate sensitivity (ECS), transient climate response (TCR), 20-year average GMSAT anomaly (2003–2022 relative to 1850–1900), aerosol effective radiative forcing (direct, indirect and total), CO_2 concentration in 2022, and ocean heat content change (2020 relative to 1971), based on the observed and assessed climate metrics taken from IPCC AR6[28] for ECS, TCR and aerosol forcing, and the Indicators of Global Climate Change 2022[55].

The same combination of EVA_H, the Marshall et al.[17]. ERF scaling and FaIR calibration has been used in Verkerk et al.[21]. Verkerk et al.[21] demonstrated that this modelling framework captures well the global mean surface cooling in response to volcanic eruptions of the last 750 years.

Simulation design

We produced 1000-member simulations for 2015–2100 (sampling the 1000-member FaIR parameter ensemble) for various combinations of future anthropogenic and volcanic forcing scenarios. For anthropogenic forcing, we used the SSP1-1.9, SSP2-4.5 and SSP5-8.5 SSP scenarios[6]. For volcanic forcing, we used:

1. The 1000 stochastic forcing scenarios generated from stochastic emission scenarios using the EVA_H model and Eq. (1) (see Method Sections "Design of stochastic volcanic emission scenarios" and "Aerosol optical properties and effective radiative forcing"). Instead of running each FaIR configuration for each volcanic forcing scenario, which would have resulted in 1,000,000 simulations per SSP scenario, we randomly pair a FaIR configuration to a stochastic volcanic forcing scenario, effectively sampling the climate uncertainty and volcanic forcing uncertainty simultaneously. We performed 1000 stochastic volcanic forcing scenarios with internal variability switched on, and 1000 stochastic volcanic forcing scenarios with internal variability switched off.
2. A control simulation with constant volcanic forcing scenario consistent with the CMIP6 ScenarioMIP recommended protocol and our modelling workflow, i.e., where the 2015–2024 global mean 550 nm SAOD is linearly ramped from its 2014 value to a value equal to that of the CMIP6 1850–2014 mean (0.010), and is then constant over 2025–2100. The corresponding forcing time series is calculated using Eq. (1).
3. Three constant volcanic forcing scenarios sampling the lower-end, middle-range and upper end of potential future emissions. To do so, we calculate using the 5th, 50th and 95th percentiles of the 2015–2100 mean global mean 550 nm SAOD distribution issued from our 1000 stochastic volcanic emission scenarios and EVA_H. The corresponding SAOD values are 0.007, 0.014 and 0.030. We then calculate volcanic forcing exactly as done for the case using the CMIP6 1850–2014 mean SAOD, including a 10-year ramp between the 2014 SAOD and the 2025–2100 constant SAOD value.

Calculation of uncertainties and probabilities

We calculated the four sources of uncertainties in climate projections as follows:

1. Scenario uncertainty - calculated using the control simulation without stochastic volcanic forcing and internal variability (no_volcanoes_future.nc) across the three SSPs (SSP1-1.9, SSP2-4.5, SSP5-8.5).

2. Model uncertainty - calculated using the control simulation without stochastic volcanic forcing and internal variability (no_volcanoes_future.nc) for one of the SSPs. The model uncertainty in our calculation does not include the influence of internal variability.
3. Volcanic uncertainty - using model simulations without internal variability, and calculated by the difference between the model simulations with and without stochastic volcanic forcing (stochastic_volcanoes.nc - no_volcanoes_future.nc).
4. Internal variability uncertainty - using model simulations without stochastic volcanic forcing, and calculated by the difference between the model simulations with and without internal variability (stochastic_volcanoes_stochastic_climate.nc - stochastic_volcanoes.nc).

To calculate the probability of exceeding warming temperature thresholds of 1.5 °C, 2 °C, and 3 °C, we calculated the number of stochastic scenarios (over the 1000 members) that exceed the temperature threshold for each year using the 30-year moving mean GMSAT values (as defined in the IPCC report).

We defined "short-term one-year GMSAT reduction" as the occurrence of a future stochastic scenario with a one-year GMSAT reduction greater than the temperature thresholds comparing to the previous year, and "short-term two-year GMSAT reduction" as the occurrence of a future stochastic scenario with two consecutive years of GMSAT reduction of at least 0.1 °C, and the two-year mean GMSAT changes greater than the temperature thresholds. We calculated the probability of short-term GMSAT reductions by counting the stochastic scenarios exceeding temperature thresholds between −0.1 °C and −0.9 °C by 2100. The probability is calculated by the difference between the FaIR model simulations with stochastic volcanic forcing and internal variability (i.e., stochastic_volcanoes_stochastic_climate.nc), and the FaIR model simulations without stochastic volcanic forcing and with internal variability (i.e., no_future_volcanoes_stochastic_climate.nc). We estimated the peak global-mean cooling of the 1991 Mt. Pinatubo eruption (18 Tg ± 5 Tg of SO_2 injection[25]) and 1815 Mt. Tambora eruption (56 Tg ± 9 Tg of SO_2 injection[11]) using the Volc2Clim webtool[25]. For the 1991 Mt. Pinatubo eruption, we assumed an uncertainty of 5 Tg of SO_2 injection. For the 1815 Mt. Tambora eruption, we assumed an uncertainty of 9 Tg of SO_2 (based on the evolv2k volcanic emission dataset). The uncertainty estimate for Tambora eruption is derived from ice core flux measurements and the uncertainties in transfer functions used to convert these ice core fluxes to stratospheric SO_2 injection values[11]. We calculated the uncertainty range of the peak global-mean surface cooing of the two eruptions using the Volc2Clim webtool with the uncertainty range of SO_2 injection stated above. We calculate the probability of at least one occurrence of short-term GMSAT increase (Supplementary Fig. S5) with a similar approach using temperature thresholds between 0.1 °C and 0.9 °C.

We designed our methodology to examine how the volcanic uncertainty related to explosive volcanic sulfur emissions affect climate projections. We did not resample the EVA_H and SAOD-ERF parameters (see Methods Section "Aerosol optical properties and effective radiative forcing") as we are not assessing the uncertainty in the conversion of volcanic emission to volcanic forcing.

Data availability
The data used in this paper is available from the University of Cambridge data repository: https://doi.org/10.17863/CAM.110898.

Code availability
FaIR v2.1.4 is available from https://github.com/OMS-NetZero/FAIR/tree/v2.1.4 as zip archives, and installable from https://anaconda.org/conda-forge/fair and https://pypi.org/project/fair/. The calibration version v1.4.2 produced for this study is available from https://doi.org/10.5281/zenodo.13142999. The code to plot the main text and Supplementary Figs. is available from https://github.com/maychim/Stochastic-volc-FAIR.

Received: 24 September 2024; Accepted: 12 March 2025;
Published online: 25 March 2025

References

1. Myhre, G. et al. Radiative forcing of the direct aerosol effect from AeroCom Phase II simulations. *Atmos. Chem. Phys.* **13**, 1853–1877 (2013).
2. Schurer, A. P., Hegerl, G. C., Mann, M. E., Tett, S. F. B. & Phipps, S. J. Separating forced from chaotic climate variability over the past millennium. *J. Clim.* **26**, 6954–6973 (2013).
3. Sigl, M. et al. Timing and climate forcing of volcanic eruptions for the past 2,500 years. *Nature* **523**, 543–549 (2015).
4. Bethke, I. et al. Potential volcanic impacts on future climate variability. *Nat. Clim. Change* **7**, 799–805 (2017).
5. Eyring, V. et al. Overview of the Coupled Model Intercomparison Project Phase 6 (CMIP6) experimental design and organization. *Geosci. Model Dev.* **9**, 1937–1958 (2016).
6. O'Neill, B. C. et al. The Scenario Model Intercomparison Project (ScenarioMIP) for CMIP6. *Geosci. Model Dev.* **9**, 3461–3482 (2016).
7. Lee, J.-Y. et al. Future global climate: scenario-based projections and near-term information. In: *Climate Change 2021: The Physical Science Basis. Contribution of Working Group I to the Sixth Assessment Report of the Intergovernmental Panel on Climate Change* (eds. Masson-Delmotte, V. et al.) 553–672 (Cambridge University Press, 2021). https://doi.org/10.1017/9781009157896.006.
8. Chim, M. M. et al. Climate projections very likely underestimate future volcanic forcing and its climatic effects. *Geophys. Res. Lett.* **50**, e2023GL103743 (2023).
9. Hawkins, E. & Sutton, R. The potential to narrow uncertainty in regional climate predictions. *Bull. Am. Meteorol. Soc.* **90**, 1095–1108 (2009).
10. Marshall, L. R. et al. Volcanic effects on climate: recent advances and future avenues. *Bull. Volcanol.* **84**, 54 (2022).
11. Toohey, M. & Sigl, M. Volcanic stratospheric sulfur injections and aerosol optical depth from 500 BCE to 1900. *Ce. Earth Syst. Sci. Data* **9**, 809–831 (2017).
12. Anchukaitis, K. J. et al. Influence of volcanic eruptions on the climate of the Asian monsoon region. *Geophys. Res. Lett.* **37**, 2010GL044843 (2010).
13. Luterbacher, J. & Pfister, C. The year without a summer. *Nat. Geosci.* **8**, 246–248 (2015).
14. Fasullo, J. T. et al. The amplifying influence of increased ocean stratification on a future year without a summer. *Nat. Commun.* **8**, 1236 (2017).
15. Gao, C., Gao, Y., Zhang, Q. & Shi, C. Climatic aftermath of the 1815 Tambora eruption in China. *J. Meteorol. Res.* **31**, 28–38 (2017).
16. Sigl, M., Toohey, M., McConnell, J. R., Cole-Dai, J. & Severi, M. Volcanic stratospheric sulfur injections and aerosol optical depth during the Holocene (past 11 500 years) from a bipolar ice-core array. *Earth Syst. Sci. Data* **14**, 3167–3196 (2022).
17. Marshall, L. R. et al. Large variations in volcanic aerosol forcing efficiency due to eruption source parameters and rapid adjustments. *Geophys. Res. Lett.* **47**, e2020GL090241 (2020).
18. Aubry, T. J., Toohey, M., Marshall, L., Schmidt, A. & Jellinek, A. M. A New Volcanic Stratospheric Sulfate Aerosol Forcing Emulator (EVA_H): Comparison With Interactive Stratospheric Aerosol Models. *J. Geophys. Res. Atmos.* **125**, e2019JD031303 (2020).
19. Leach, N. J. et al. FaIRv2.0.0: a generalized impulse response model for climate uncertainty and future scenario exploration. *Geosci. Model Dev.* **14**, 3007–3036 (2021).
20. Smith, C. J. et al. fair-calibrate v1.4.1: calibration, constraining and validation of the FaIR simple climate model for reliable future climate projections. *Geosci. Model Dev.* **17**, 8569–8592 (2024).

21. Verkerk, M. et al. Using reduced-complexity volcanic aerosol and climate models to produce large ensemble simulations of Holocene temperature. *EGUsphere* **2024**, 1–33 (2024).
22. van Vuuren, D. et al. The Scenario Model Intercomparison Project for CMIP7. Preprint at https://doi.org/10.5194/egusphere-2024-3765 (2025).
23. Betts, R. A. et al. Approaching 1.5 °C: how will we know we've reached this crucial warming mark? *Nature* **624**, 33–35 (2023).
24. Forster, P. M. et al. Indicators of global climate change 2023: annual update of key indicators of the state of the climate system and human influence. *Earth Syst. Sci. Data* **16**, 2625–2658 (2024).
25. Schmidt, A., Aubry, T., Rigby, R., Stevenson, J. A. & Loughin, S. Volc2Clim online tool. *Zenodo* https://doi.org/10.5281/ZENODO.7602062 (2023).
26. Mulcahy, J. P. et al. UKESM1.1: development and evaluation of an updated configuration of the UK Earth System Model. *Geosci. Model Dev.* **16**, 1569–1600 (2023).
27. Clyne, M. et al. Model physics and chemistry causing intermodel disagreement within the VolMIP-Tambora Interactive Stratospheric Aerosol ensemble. *Atmos. Chem. Phys.* **21**, 3317–3343 (2021).
28. Forster, P. M. et al. The Earth's energy budget, climate feedbacks, and climate sensitivity. In: *Climate Change 2021: The Physical Science Basis. Contribution of Working Group I to the Sixth Assessment Report of the Intergovernmental Panel on Climate Change* (eds. Masson-Delmotte, V. et al.) 923–1054 (Cambridge University Press, 2021). https://doi.org/10.1017/9781009157896.009.
29. Nicholls, Z. R. J. et al. Reduced complexity model intercomparison project phase 1: introduction and evaluation of global-mean temperature response. *Geosci. Model Dev.* **13**, 5175–5190 (2020).
30. Cassidy, M. & Mani, L. Huge volcanic eruptions: time to prepare. *Nature* **608**, 469–471 (2022).
31. Aubry, T. J. et al. Climate change modulates the stratospheric volcanic sulfate aerosol lifecycle and radiative forcing from tropical eruptions. *Nat. Commun.* **12**, 4708 (2021).
32. Carn, S. Multi-Satellite Volcanic Sulfur Dioxide L4 Long-Term Global Database V4 (MSVOLSO2L4 4), https://disc.gsfc.nasa.gov/datasets/MSVOLSO2L4_4/summary (2022).
33. Global Volcanism Program. Volcanoes of the World, v.5. Global Volcanism Program https://doi.org/10.5479/si.GVP.VOTW5-2022.5.0 (2022).
34. Fero, J., Carey, S. N. & Merrill, J. T. Simulating the dispersal of tephra from the 1991 Pinatubo eruption: Implications for the formation of widespread ash layers. *J. Volcanol. Geotherm. Res.* **186**, 120–131 (2009).
35. Aubry, T. J. et al. Impact of climate change on volcanic processes: current understanding and future challenges. *Bull. Volcanol.* **84**, 58 (2022).
36. Aubry, T. J. et al. Impact of global warming on the rise of volcanic plumes and implications for future volcanic aerosol forcing. *J. Geophys. Res. Atmos.* **121**, 13,326–13,351 (2016).
37. Neely, R. R. I. & Schmidt, A. VolcanEESM: Global volcanic sulphur dioxide (SO2) emissions database from 1850 to present - Version 1.0. NERC Centre for Environmental Data Analysis (CEDA) https://doi.org/10.5285/76EBDC0B-0EED-4F70-B89E-55E606BCD568 (2016).
38. Sigl, M., Toohey, M., McConnell, J. R., Cole-Dai, J. & Severi, M. HolVol: Reconstructed volcanic stratospheric sulfur injections and aerosol optical depth for the Holocene (9500 BCE to 1900 CE). https://doi.org/10.1594/PANGAEA.928646 (2021).
39. Fang, S.-W. et al. The role of small to moderate volcanic eruptions in the early 19th century climate. *Geophys. Res. Lett.* **50**, e2023GL105307 (2023).
40. Toohey, M., Stevens, B., Schmidt, H. & Timmreck, C. Easy Volcanic Aerosol (EVA v1.0): an idealized forcing generator for climate simulations. *Geosci. Model Dev.* **9**, 4049–4070 (2016).
41. Zanchettin, D. et al. The Model Intercomparison Project on the climatic response toVolcanic forcing (VolMIP): experimental design and forcing input data for CMIP6. *Geosci. Model Dev.* **9**, 2701–2719 (2016).
42. Jungclaus, J. H. et al. The PMIP4 contribution to CMIP6 – Part 3: The last millennium, scientific objective, and experimental design for the PMIP4 past1000 simulations. *Geosci. Model Dev.* **10**, 4005–4033 (2017).
43. Vernier, J.-P. et al. The 2019 raikoke eruption as a testbed used by the volcano response group for rapid assessment of volcanic atmospheric impacts. *Atmos. Chem. Phys.* **24**, 5765–5782 (2024).
44. Schmidt, A. et al. Volcanic radiative forcing from 1979 to 2015. *J. Geophys. Res. Atmos.* **123**, 12491–12508 (2018).
45. Myhre, G. et al. Anthropogenic and natural radiative forcing. In: *Climate Change 2013: The Physical Science Basis. Contribution of Working Group I to the Fifth Assessment Report of the Intergovernmental Panel on Climate Change*. (Cambridge University Press, 2014). https://doi.org/10.1017/CBO9781107415324.018.
46. Smith, C. J. et al. FAIR v1.3: a simple emissions-based impulse response and carbon cycle model. *Geosci. Model Dev.* **11**, 2273–2297 (2018).
47. Millar, R. J. et al. Emission budgets and pathways consistent with limiting warming to 1.5 °. *C. Nat. Geosci.* **10**, 741–747 (2017).
48. Smith, C. J. & Mathison, C. How much methane removal is required to avoid overshooting 1.5 °C? *Environ. Res. Lett.* **19**, 074044 (2024).
49. Smith, C. J. et al. Energy budget constraints on the time history of aerosol forcing and climate sensitivity. *J. Geophys. Res. Atmos.* **126**, e2020JD033622 (2021).
50. Hodnebrog, Ø. et al. Updated global warming potentials and radiative efficiencies of halocarbons and other weak atmospheric absorbers. *Rev. Geophys.* **58**, e2019RG000691 (2020).
51. Smith, C. J. & Forster, P. M. Suppressed late-20th century warming in CMIP6 models explained by forcing and feedbacks. *Geophys. Res. Lett.* **48**, e2021GL094948 (2021).
52. Thornhill, G. D. et al. Effective radiative forcing from emissions of reactive gases and aerosols – a multi-model comparison. *Atmos. Chem. Phys.* **21**, 853–874 (2021).
53. Thornhill, G. D. et al. Climate-driven chemistry and aerosol feedbacks in CMIP6 Earth system models. *Atmos. Chem. Phys.* **21**, 1105–1126 (2021).
54. Cummins, D. P., Stephenson, D. B. & Stott, P. A. Optimal estimation of stochastic energy balance model parameters. *J. Clim.* **33**, 7909–7926 (2020).
55. Forster, P. M. et al. Indicators of global climate change 2022: annual update of large-scale indicators of the state of the climate system and human influence. *Earth Syst. Sci. Data* **15**, 2295–2327 (2023).
56. Smith, C. J. FaIR calibration data v1.4.2. *Zenodo*, https://doi.org/10.5281/ZENODO.13142999 (2024).
57. Nicholls, Z. R. J. et al. Reduced complexity model intercomparison project phase 2: synthesizing earth system knowledge for probabilistic climate projections. *Earths Fut.* **9**, e2020EF001900 (2021).
58. Smith, C. J. et al. The Earth's energy budget, climate feedbacks, and climate sensitivity Supplementary Material. In: *Climate Change 2021: The Physical Science Basis. Contribution of Working Group I to the Sixth Assessment Report of the Intergovernmental Panel on Climate Change* (Cambridge University Press, 2021).

Acknowledgements

M.M.C. is supported by the Croucher Foundation and The Cambridge Commonwealth, European & International Trust through a Croucher Cambridge International Scholarship, and the Joseph Needham Foundation for Science and Civilisation through a Joseph Needham Merit Scholarship. M.M.C. and T.J.A. acknowledge support from the Camborne School of Mines Trust International Travel Bursary and the Department of Earth and Environmental Sciences of the University of Exeter. T.J.A. acknowledges funding from the Coupled Model Intercomparison Project International Project Office (PO 4000136906) and the European Space Agency (Project "Volcanic Forcing for CMIP", contract number 4000145911/24/I-LR). C.S. was funded by a NERC/IIASA Collaborative Research Fellowship (NE/T009381/1) and Horizon Europe under Grant Agreements 101081369 (SPARCCLE) and 101081661 (WorldTrans).

Author contributions
T.J.A. and A.S. conceived the study with feedback from M.M.C. and C.S. M.M.C. generated the stochastic volcanic emission scenarios. T.J.A. performed the EVA_H runs to generate the stochastic volcanic forcing scenarios. C.S. performed the FaIR model simulations. M.M.C. performed the analysis and data visualisation. M.M.C. wrote the first draft of the article with the contributions from T.J.A., C.S., and A.S. All the authors contributed to the interpretation of the results and refinement of the article.

Competing interests
The authors declare no competing interests.

Additional information
Supplementary information The online version contains supplementary material available at https://doi.org/10.1038/s43247-025-02208-1.

Correspondence and requests for materials should be addressed to Man Mei Chim.

Peer review information *Communications Earth & Environment* thanks the anonymous reviewers for their contribution to the peer review of this work. Primary Handling Editors: Mengze Li and Alireza Bahadori. A peer review file is available.